minimize blowing and suction at the gaps, both drag and heat-transfer tests operated a vacuum system in the plenum chamber enclosing the test section in order to match the static pressure below the drag balance or heater plate support with that of the test section. The rear side wall was adjusted in both sets of measurements to actively maintain a near-zero pressure gradient in the test section. Careful model alignment and calibration checks insured drag data repeatability to within $\pm 1\%$. Skin-friction coefficients were backed out from direct drag measurements using the following relation:

$$D = \tfrac{1}{2} A C_f \rho_\infty U_\infty^2$$

Results and Discussion

The LEBU heat-transfer coefficients were generally depressed (6% maximum reduction) below flat-plate values. See Table 2 for test heat-transfer data. The three-LEBU stacks produced the lowest heat-transfer coefficients for the two sets of tripped flows. As U_∞ and Re_θ increase, the test heat-transfer coefficients for a given stack configuration decrease, while the flat-plate reference coefficients remain stable throughout the test speed range. In fact, all flat-plate heat-transfer coefficients for both rod and screen trips were roughly equivalent to within experimental error. It is particularly interesting to note that if the scatter in the screen-tripped heat-tansfer data were merely a phenomenon of experimental error, then it does not appear that the screen-tripped heat-transfer data were a function of velocity. In contrast, while the rod-tripped heat-transfer data are monotonic, that data may well be velocity- and/or Re_θ-dependent (lower Re_θ, post-transitional flow).

Drag data for the LEBUs agree in trend to previous data in similar configurations and test conditions.[1,2,6] (See Table 2 for test drag data.) The three-LEBU stack yielded average C_f reductions of up to 13% (screen trip only) and consistently exhibited the greatest average C_f reductions of all the LEBU configurations for both sets of tripped flows. (Note that the recorded experimental average C_f reductions do not include the penalty of device drag.) The reductions associated with the screen trip and higher Reynolds numbers are significantly greater than with the two-dimensional rod trip (transitional flow effects[2]). Note that, unlike the heat-transfer cases, the drag results remain markedly stable for a given configuration throughout the test speed range.

Because the overall C_f reductions exceed the heat-transfer coefficient reductions, the relative Reynolds analogy factors (here constructed in terms of the simple efficiency relation η) are somewhat increased above (average increase approximately 7%) the appropriate flat-plate reference. Again refer to Table 2 for measured relative LEBU Reynolds analogy factors. The two-LEBU stacks exhibit the highest Reynolds analogy factors for both sets of tripped flows. Reynolds analogy factors tend to decrease as U_∞ increases per each LEBU stack; other trends, if any, are difficult to identify.

The fact that LEBUs heat transfer is reduced is not surprising for several reasons: LEBUs tend to reduce the vertical component (primary heat-transfer direction) of large-scale motion[1] and insertion of LEBUs causes a redistribution of fine-scale turbulence in place of large, more uneven structures (inherently better carriers of thermal energy differentials).[2] Reynolds analogy factors for LEBUs, however, are generally elevated above flat-plate values, which means that the C_f reduction is greater than the corresponding heat-transfer reduction. This suggestion also makes sense in the light of such experimental observations that: 1) the wall law similarity is re-established early for $y/\delta_{SL} > 0.3$, (i.e., forecasting nominal heat-transfer reduction), although C_f reductions persist;[3] and 2) for 30% LEBU C_f reduction, the sublayer is increased 17% (i.e., turbulent heat-transfer reduction conceivably closer to 17%).

In addition to the above results, the variation in stability of the LEBU heat-transfer and skin-friction data throughout the test speed range also suggests that independent mechanisms influence the two flow parameters. In support of this interpretation, a growing body of experimental data offers evidence that, contrary to the similarity imposed by standard Reynolds analogy models, heat transfer and skin friction are affected differently in situations characterized by surface roughness or curvature, physical or thermal steps, and pressure gradients.

References

[1]Corke, T.C., Nagib, H.M., and Guezennec, Y.G., "A New View on Origin, Role and Manipulation of Large Scales in Turbulent Boundary Layers," NASA CR-165861, Feb. 1982.

[2]Anders, J.B., Hefner, J.N., and Bushnell, D.M., "Performance of Lage-Eddy Breakup Devices at Post-Transitional Reynolds Numbers," AIAA Paper 84-0345, Jan. 1984.

[3]Nguyen, V.D., Dickinson, J., Lemay, A.J., Haeberle, D., Larose, G., Boisvert, L.M., Chalifour, Y., and Jean, Y., "Some Experimental Observations of the Law of the Wall Behind Large-Eddy Breakup Devices Using Servo-Controlled Skin Friction Balances," AIAA Paper 84-0346, Jan. 1984.

[4]Nguyen, V.D., Dickinson, J., Lemay, J., Provencal, D., Jean, Y., and Chalifour, Y., "The Determination of Turbulent Skin Friction Behind Flat Plate Turbulence Manipulators Using Servo-Controlled Balances," *Proceedings of the International Council of the Aeronautical Sciences Congress XIV,* Vol. 1, 1984, pp. 404-409.

[5]Mumford, J.C. and Savill, A.M., "Parametric Studies of Flat Plate, Turbulence Manipulators Including Direct Drag Results and Laser Flow Visualization" *Laminar and Turbulent Boundary Layers, Proceedings of the Energy Sources Technology Conference,* Rolls Royce, 1984, pp. 41-51.

[6]Bandyopadhyay, P.R., "The Performance of Smooth-Wall Drag Reducing Outer-Layer Devices in Rough-Wall Boundary Layers," AIAA Paper 85-0558, March 1985.

[7]Lindemann, A.M., "Turbulent Reynolds Analogy Factors for Nonplanar Surface Microgeometries," *Journal of Spacecraft and Rockets,* Vol. 22, Sept.-Oct. 1985, pp. 581-582.

Analyses of Spacecraft Polymeric Materials

S. D. Worley,* C. H. Dai,† J. L. Graham,†
A. T. Fromhold,† and K. Daneshvar§
Auburn University, Auburn, Alabama
and
A. F. Whitaker¶ and S. A. Little**
Marshall Space Flight Center, Huntsville, Alabama

Introduction

IT has been recognized since the pioneering work of Leger[1] concerning materials exposed on missions STS-1 through STS-3 and of Hansen and coworkers[2] in a ground-based study that LEO atomic oxygen may present a serious problem for materials used in conjuction with the space telescope. Atomic oxygen is the major ambient species at low orbital altitudes and presents a flux of *ca.* 8×10^{14} atoms cm^{-2} s^{-1} for oxidative reaction with materials.[1] Leger observed a significant alteration in appearance of the Kapton

Received Aug. 2, 1985; revision received Dec. 16, 1985.

*Alumni Professor of Chemistry.
†Graduate Student, Chemistry.
‡Professor of Physics.
§Assistant Professor of Electrical Engineering.
¶Deputy Chief, Engineering Physics Division. Member AIAA.
**Physicist, Physical Sciences Branch.

film used on the television camera thermal blanket, but the analytical techniques employed (MIR, SEM, and ESCA) showed no significant surface contaminant.[1] Whitaker has discussed the effects of LEO atomic oxygen on several materials exposed on mission STS-5; considerable material[1] weight loss was observed for Kapton.[3] Whitaker and coworkers have also discussed the degradation of various materials during mission STS-8.[4]

The purpose of this Note is to address partial analytical characterization by four techniques of three polymeric materials used in conjunction with the space telescope for samples flown on mission STS-8.

Experimental

Transmission infrared (IR) measurements were performed on thin films of the three materials (white Tedlar, Kapton H, and Kapton F), using a Perkin-Elmer 983 spectrometer equipped with a data system for subtraction of spectra. X-ray photoelectron spectra (XPS) were obtained for the three materials using an LHS10 Leybold-Haraeus spectrometer with 1487 eV AlKα radiation as the excitation source impinging at a 30-deg angle. For the XPS work, the samples were cut into 1-cm "bone-shaped" specimens which were mounted in molybdenum boats fabricated to fit the sample rod for the spectrometer. A strand of gold wire was wrapped around the samples to hold them in place in the boats as well as to provide a calibration material. The XPS band positions for Au are well documented, although there has been considerable recent controversy concerning the suitability of Au as an internal calibrant, especially for insulating materials.[5] Proton-induced X-ray emission (PIXE) data were obtained using a 3 MeV Dynamtron Ion Accelerator at Auburn University. The ellipsometry measurements were made with a Gaertner L119 ellipsometer.

The samples (controls and flight) of white Tedlar, Kapton H, and Kapton F were cut in disks measuring 25 mm in diam with a thickness of 0.025 mm. The flight samples were vacuum degassed and mounted in disk holders on a tray for the STS-8 mission. The flight samples were subjected to an incident atomic oxygen total fluence of 3.5×10^{20} atoms cm^{-2} at a temperature interval of $10\pm10°C$ for 41.17 h at 120 n.m. during the mission. The control samples were not flown on the mission, but otherwise treated identically to the flight samples. There was no evidence of surface contamination (such as oxidized silicone) detected (XPS) for any of the samples.

Results and Discussion

Typical transmission IR spectra for the white Tedlar mission sample and a control sample are shown in Fig. 1. There is little difference between the two spectra; this was the case also for the Kapton H and F samples. Since transmission IR should detect chemical and structural changes throughout the bulk of the samples, any damage to the films must have been confined to the outermost (surface) layers. Such surface damage would not be detected by transmission IR because the molecules present near the surface represent a negligible percentage as compared to the bulk. It can be concluded that transmission IR is probably not a very useful technique for studying damage to materials in space, except as proof that the damage is confined to the surface.

The XPS measurements in this study provided the most useful data for the three types of samples. It is well-known that XPS probes the outermost 20-50 Å of material, and is thus a good surface analytical technique. Typical XPS in the C(1s) binding energy region for white Tedlar are shown in Fig. 2. White Tedlar contains the elements H, F, and C in a repeating unit of $(-CH_2CHF-)_n$;[6] thus there are two inequivalent C atoms present. The spectra in Fig. 2 show three C(1s) XPS bands having binding energies (eV) of control (shuttle): 290.0(291.5), 287.2(289.4), and 285.4(285.4). The band at 285.4 eV, which does not shift upon exposure to the environment of space, corresponds to C contamination on the gold wire. The other two C(1s) bands, which do shift to higher binding energy upon exposure to space, refer to the

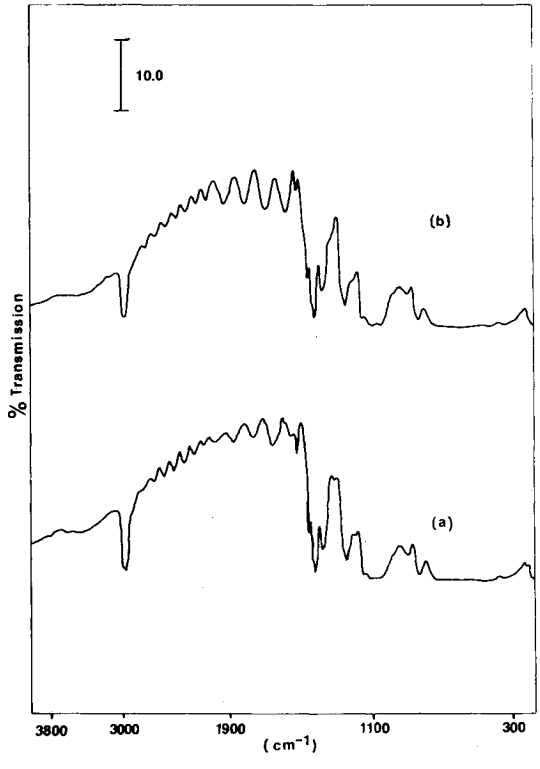

Fig. 1 Transmission infrared spectra of white Tedlar disks: a) unexposed to atomic oxygen (control); b) exposed to atomic oxygen during the STS-8 mission.

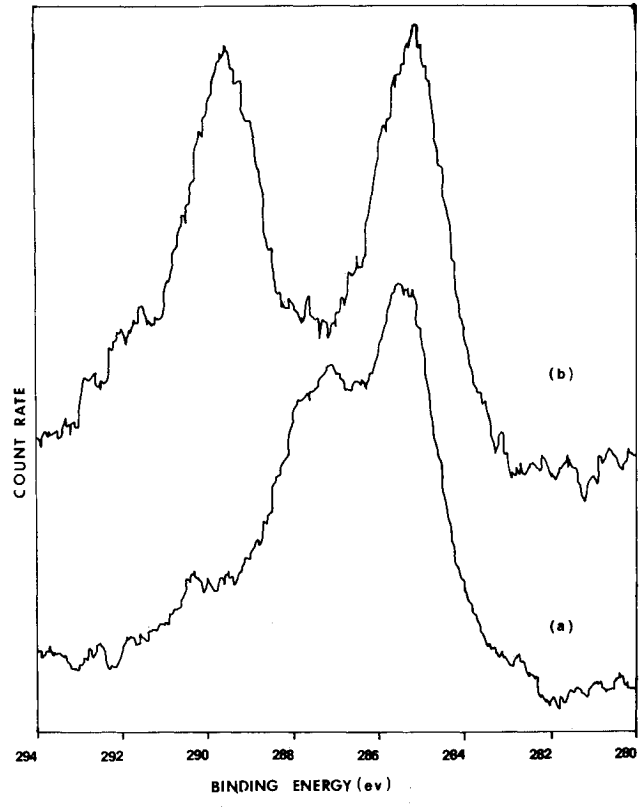

Fig. 2 X-ray photoelectron spectra in the C(1s) binding energy region of white Tedlar disks: a) unexposed to atomic oxygen (control); b) exposed to atomic oxygen during the STS-8 mission.

two inequivalent C atoms in the white Tedlar polymer. That they shift to substantially higher binding energy demonstrates that the surface was oxidized during flight, probably by atomic oxygen. This could indicate conversion of C to a more highly oxidized state of C, e.g., a carbonyl group, or possibly merely to the implantation of atomic oxygen near the C in its molecular environment. An intense O(1s) band near 536 eV was obtained for the mission sample, but not for the control. This again indicates implanted oxygen during the flight. The F(1s) band at 690.4 eV was shifted to higher binding energy for the exposed shuttle sample relative to the unexposed control (688.7 eV) also indicating oxidation of the white Tedlar surface.

The XPS data for the two Kapton samples are more complex because of the nature of the polymers. The Kapton H polymer contains a repeating unit of $(C_{22}H_{10}N_2O_5)_n$ with seven inequivalent C atoms and two inequivalent O atoms.[6] Kapton F has a Teflon coating, and as such, its XPS should be that of Teflon. However, the XPS of the Kapton H film clearly indicate oxidation of the surface during the shuttle flight, because all bands shifted to higher binding energy for the exposed flight sample relative to the control. That the X-ray beam did not penetrate the Teflon layer of Kapton F is illustrated by the fact that no N(1s) band could be obtained for this sample, while one was clearly evident for the Kapton H sample. It is very interesting that the C(1s) bands for Kapton F (Teflon) both shifted to *lower* binding energy for the exposed shuttle sample vs the unexposed control. This must indicate that fluorine atoms are removed from the sample in space due to bombardment by atomic oxygen. Since F is more electronegative than O, such would explain the shift to lower binding energy for Kapton F.

The PIXE measurements were used to determine the elemental concentration change of the exposed shuttle samples relative to the control samples. This technique is not suitable for elements with lower atomic number than F; thus no useful data was obtained for Kapton H. However, Kapton F definitely showed a loss of F for the exposed flight sample supporting our XPS conclusion noted earlier. The white Tedlar contained Na, Si, and V as impurities; all of these as well as F were reduced in the exposed flight sample relative to the control. The ellipsometry data obtained in this study showed a factor of two decrease in absorption coefficient upon comparison of the control and exposed flight sample for Kapton H. This again indicates surface damage to the material.

Conclusions

The following conclusions can be drawn from this study: 1) The surfaces of the three polymers were attacked and oxidized by atomic oxygen; 2) fluorine is lost from the surface of Kapton F, probably due to displacement by atomic oxygen.

Acknowledgment

The authors wish to thank NASA through the Marshall Space Flight Center for partial support (Contract NAS8-35914) of this work.

References

[1]Leger, L. J., "Oxygen Atom Reaction with Shuttle Materials at Orbital Altitudes," NASA Tech. Memo. 58246, May 1982.

[2]Hansen, R., Pascale, J., DeBenedictis, T., and Rentzepis, P., "Effect of Atomic Oxygen on Polymers," *Journal Polymer Science,* Vol. 3, June 1965, pp. 2205-2214.

[3]Whitaker, A. F., "LEO Atomic Oxygen Effects on Spacecraft Materials," AIAA Conference on Shuttle Environments and Operations, Oct. 1983.

[4]Whitaker, A. F., Little, S. A., Harwell, R. J., Griner, D. B., DeHaye, R., F., and Fromhold, A. T., "Orbital Atomic Oxygen Effects on Thermal Control and Optical Materials—STS-8 Results," AIAA Paper 85-0416, Jan. 1985.

[5]Kohiki, S. and Oki, K., "An Appraisal of Evaporated Gold as an Energy Reference in X-ray Photoelectron Spectroscopy," *Journal of Electron Spectroscopy and Related Phenomena,* Vol. 36, May 1985, pp. 105-110, and references cited therin.

[6]Hawley, G. G., *The Condensed Chemical Dictionary*, 8th ed., Van Nostrand Reinhold Company, New York, 1971, pp. 714, 848.

[7]NBS Monograph 132, Sept. 1973.